The major factors affecting the tacticity include the symmetry of the catalyst dictated by the steric environment of the ancillary ligands. Olefin complexation occurs with the methyl group being placed in the least sterically congested quadrant, and this process continues, ultimately determining the stereochemistry of the growing polymer chain. This lends further support to enantiomorphic site control of chirality. Since there is an energetic differential between the first insertion (3 kcal/mol) and subsequent insertions (5 to 6 kcal/mol), the isotacticity is at least partially due to a double stereodifferentiation.[12c]

Acknowledgment. We thank Molecular Simulations Inc., for the use of the Biograf and Polygraf molecular simulation programs. Parital support of this research by Shell Development is gratefully acknowledged. This research was partially supported by a grant (GM39038) from the National Institutes of Health. A.K.R. gratefully acknowledges helpful discussions with Drs. W. M. Skiff, S. E. Wilson, and P. N. Haxin of Shell Development.

Design of Chromophoric Molecular Assemblies with Large Second-Order Optical Nonlinearities. A Theoretical Analysis of the Role of Intermolecular Interactions

Santo Di Bella,† Mark A. Ratner,* and Tobin J. Marks*

Contribution from the Department of Chemistry and the Materials Research Center, Northwestern University, Evanston, Illinois 60208-3113. *Received December 30, 1991*

Abstract: The role and nature of intermolecular interactions in determining quadratic nonlinear optical macroscopic hyperpolarizabilities are investigated using the INDO/S (ZINDO) sum-over excited particle-hole-states formalism on clusters (dimers and trimers) of archetypical donor/acceptor organic π-electron chromophore molecules. It is found that the calculated aggregate hyperpolarizability depends strongly on relative molecular orientations, exhibiting the largest values in slipped cofacial arrangements, where the donor substituent of one molecular unit is in close spatial proximity to the acceptor substituent of the nearest neighbor. These results convey important suggestions for the design of multichromophore assemblies having optimum $\chi^{(2)}$ values. For example, cofacial assembly of chromophores having low ground-state dipole moments should maximize molecular contributions to the macroscopic susceptibility. The classical "two-level" model is a good approximation for estimating the hyperpolarizability in such cluster systems, although at larger distances it yields overestimated β_{ijk} values. Other cases where the two-level model breaks down more significantly are also identified.

Introduction

Materials exhibiting large nonlinear optical (NLO) responses, in particular those composed of conjugated organic chromophore molecules, have attracted much recent scientific interest.[1-3] The attraction of incorporating them into devices for technological applications has stimulated efforts in the design and synthesis of new chromophoric building blocks and multimolecular assemblies.[2,3] The concurrent desirability of having a proper, chemically-oriented, physical description of molecular NLO phenomena has led to the parallel development of quantum chemical approaches for calculating optical nonlinearities.[4-7] To date these approaches have, however, been largely limited to the calculation of the *molecular* nonlinear response in order to rationalize and optimize single chromophore quadratic hyperpolarizabilities.[4-7] The important relationship between microscopic and macroscopic second-order NLO properties has only been addressed for macroscopic systems (e.g., crystals,[8] poled polymers,[9] assembled layer thin films[10]) using local field factor corrections that phenomenologically approximate, via empirical polarizabilities, molecule–molecule interactions and the effects of molecular packing on the molecular hyperpolarizability.[11-14]

An alternative computational approach for estimation of nonadditive interchromophore effects would be to consider a molecular cluster representative of the crystal environment to calculate the effective hyperpolarizability. In this case, in place of electrostatic corrections, it should be possible to define, via reliable electronic structure formalism, the role and nature of intermolecular interactions that determine the bulk hyperpolarizability and ultimately to use this information for the design of new materials. The aims of the present work are to explore systematically, for the first time in any detail,[15] the second-order nonlinear response of simple clusters (dimers and trimers) of

† Permanent address: Dipartimento di Scienze Chimiche, Universitā di Catania, 95125 Catania, Italy.

(1) (a) Boyd, R. W. *Nonlinear Optics*; Academic Press: New York, 1992. (b) Prasad, N. P.; Williams, D. J. *Introduction to Nonlinear Optical Effects In Molecules and Polymers*; Wiley: New York, 1991. (c) Shen, Y. R. *The Principles of Nonlinear Optics*; Wiley: New York, 1984.

(2) (a) *Materials for Nonlinear Optics: Chemical Perspectives*; Marder, S. R., Sohn, J. E., Stucky, G. D., Eds.; ACS Symposium Series 455; American Chemical Society: Washington, DC, 1991. (b) *Nonlinear Optical Properties of Organic Materials III*; Khanarian, G., Ed. *SPIE Proc.* **1990**, *1337*. (c) *Nonlinear Optical Properties of Organic Materials II*; Khanarian, G., Ed. *SPIE Proc.* **1990**, *1147*. (d) *Nonlinear Optical Effects in Organic Polymers*; Messier, J., Kajar, F., Prasad, P., Ulrich, D., Eds.; Kluwer Academic Publishers: Dordrecht, 1989. (e) *Organic Materials for Nonlinear Optics*; Hann, R. A., Bloor, D., Eds.; Royal Society of Chemistry: London, 1988. (f) *Nonlinear Optical Properties of Organic Molecules and Crystals*; Chemla, D. S., Zyss, J., Eds.; Academic Press: New York, 1987; Vols. 1 and 2. (g) *Nonlinear Optical Properties of Organic and Polymeric Materials*; Williams, D. J., Ed.; ACS Symposium Series 233; American Chemical Society: Washington, DC, 1984.

(3) (a) Eaton, D. F. *Science* **1991**, *253*, 281. (b) Marder, S. R.; Beratan, D. N.; Cheng, L.-T. *Science* **1991**, *252*, 103. (c) Zyss, J. *J. Mol. Electron.* **1985**, *1*, 25. (d) Williams, D. J. *Angew. Chem., Intl. Ed. Engl.* **1984**, *23*, 690.

(4) Ab initio: (a) Karna, S. P.; Prasad, P. N.; Dupuis, M. *J. Chem. Phys.* **1991**, *94*, 1171. (b) Meyers, F.; Adant, C.; Bredas, J. L. *J. Am. Chem. Soc.* **1991**, *113*, 3715. (c) Rice, J. E.; Amos, R. D.; Colwell, S. M.; Handy, N. C.; Sanz, J. *J. Chem. Phys.* **1990**, *93*, 8828. (d) Dykstra, C. E.; Jasien, P. G. *Chem. Phys. Lett.* **1984**, *109*, 388. (e) Sekino, H.; Bartlett, R. J. *J. Chem. Phys.* **1986**, *85*, 976; *Int. J. Quantum Chem.*, in press.

(5) CNDO/S: (a) Morley, J. O. *J. Chem. Soc., Faraday Trans.* **1991**, *87*, 3009, 3015. (b) Morley, J. O. *J. Am. Chem. Soc.* **1988**, *110*, 7660. (c) Docherty, V. J.; Pugh, D.; Morley, J. O. *J. Chem. Soc., Faraday Trans. 2* **1985**, *81*, 1179. (d) Lalama, S. J.; Garito, A. F. *Phys. Rev.* **1979**, *20*, 1179. (e) Morrell, J. A.; Albrecht, A. C. *Chem. Phys. Lett.* **1979**, *64*, 46.

(6) PPP: (a) Li, D.; Ratner, M. A.; Marks, T. J. *J. Phys. Chem.*, in press. (b) Li, D.; Ratner, M. A.; Marks, T. J. *J. Am. Chem. Soc.* **1988**, *110*, 1707. (c) Li, D.; Marks, T. J.; Ratner, M. A. *Chem. Phys. Lett.* **1986**, *131*, 370. (d) Dirk, C. W.; Twieg, R. J.; Wagniere, G. *J. Am. Chem. Soc.* **1986**, *108*, 5387. (e) Soos, Z.; Ramasesha, S. *J. Chem. Phys.* **1989**, *90*, 1067.

0002-7863/92/1514-5842$03.00/0

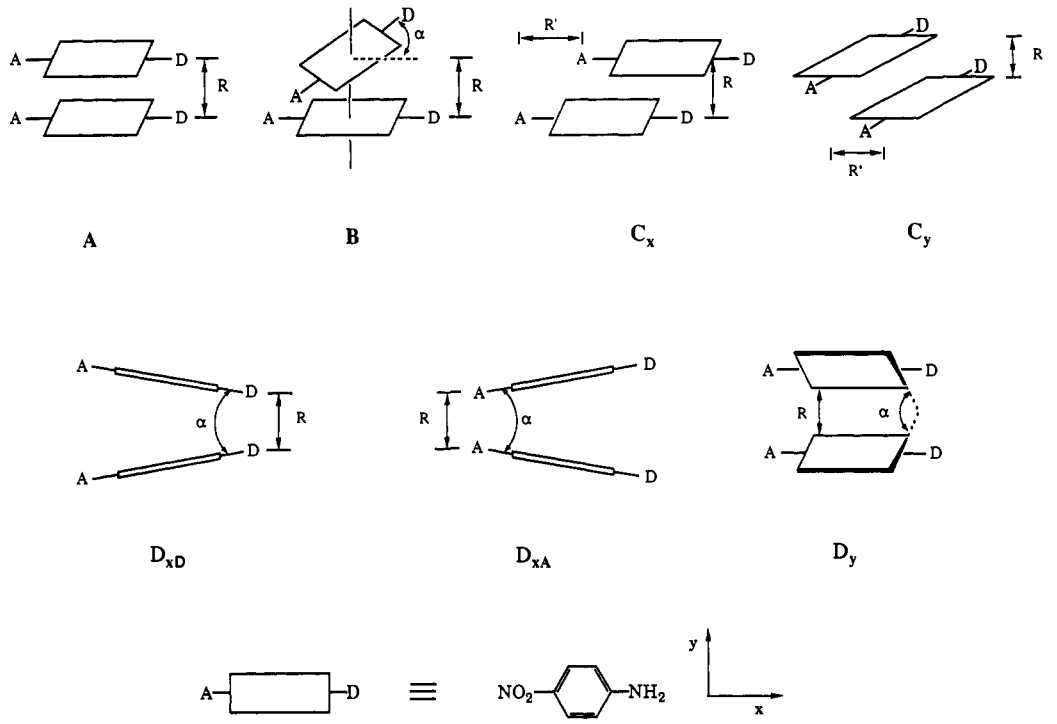

Figure 1. Molecular geometries of the PNA (*p*-nitroaniline) dimer examined. Eclipsed (A), staggered (B), slipped (C), and tilted (D) conformations.

selected chromophoric NLO subunits placed in various relative orientations, to relate the resulting intermolecular interactions to the macroscopic/quadratic hyperpolarizabilities, and to identify those among the various possible packing geometries that will afford the maximum macroscopic second-order nonlinear susceptibility $\chi^{(2)}$.

In this contribution, we report a theoretical analysis using the ZINDO-SOS formalism[7a-c] of the cases of clusters (dimers and trimers) formed by monomeric units of archetypical chromophore molecules having donor (D) and acceptor (A) substituents connected by a conjugated pathway, (e.g., *p*-nitroaniline, PNA, **1**).

1 **2**

These results are then compared to a cluster constructed from a chromophore with a nearly vanishing molecular dipole moment such as 3-methyl-4-nitropyridine 1-oxide[16] (POM, **2**), thereby probing the role of different types of intermolecular interactions in determining the nonlinear optical response. It will be seen that this approach is of general applicability and may be extended to a variety of other multimolecular NLO systems. The ZINDO-INDO/S formalism is of proven reliability in the description of molecular linear[17] and nonlinear[7] optical phenomena as well as of linear spectroscopic response to various intermolecular interactions.[18]

Computational Details

The Sum-Over excited particle-hole-States (SOS) formalism,[19] in connection with the all-valence INDO/S (Intermediate Neglect of Differential Overlap) technique,[17] was employed. The details of the ZINDO-SOS-based method for describing second-order molecular optical nonlinearities have been reported elsewhere.[7a-c] Standard parameters and basis functions were used. In the present approach, the single-determinant, molecular orbital approximate ground state was used, and the monoexcited configuration interaction (MECI) approximation was employed to describe the excited states. In computations of PNA dimers,

(7) INDO/S: (a) Kanis, D. R.; Marks, T. J.; Ratner, M. A. *Int. J. Quantum Chem.*, in press. (b) Kanis, D. R.; Ratner, M. A.; Marks, T. J.; Zerner, M. C. *Chem. Mat.* **1991**, *3*, 19. (c) Kanis, D. R.; Ratner, M. A.; Marks, T. J. *J. Am. Chem. Soc.* **1990**, *112*, 8203. (d) Parkinson, W. A.; Zerner, M. C. *J. Chem. Phys.* **1991**, *94*, 478. (e) Ulman, A.; Willand, C. S.; Kohler, W.; Robello, D. R.; Williams, D. J.; Handley, L. *J. Am. Chem. Soc.* **1990**, *112*, 7083. (f) Kanis, D. R.; Marks, T. J.; Ratner, M. A. *J. Am. Chem. Soc.*, submitted for publication.

(8) (a) Zyss, J.; Oudar, J. L. *Phys. Rev. A* **1982**, *26*, 2028. (b) Oudar, J. L.; Zyss, J. *Phys. Rev. A* **1982**, *26*, 2016.

(9) (a) Singer, K. D.; Kuzyk, M. G.; Sohn, J. E. *J. Opt. Soc. Am. B* **1987**, *4*, 968. (b) Williams, D. J. In *Nonlinear Optical Properties of Organic Molecules and Crystals*; Chemla, D. S., Zyss, J., Eds.; Academic Press: New York, 1987; Vol. 1, p 405. (c) Meredith, G. R.; Vandusen, J. G.; Williams, D. J. In *Nonlinear Optical Properties of Organic and Polymeric Materials*; Williams, D. J., Ed.; ACS Symposium Series 233; American Chemical Society: Washington, DC, 1984; p 109.

(10) (a) Shen, Y. R. *Annu. Rev. Phys. Chem.* **1989**, *40*, 327. (b) Shen, Y. R. In *Organic Materials for Nonlinear Optics*; Hann, R. A., Bloor, D., Eds.; Royal Society of Chemistry: London, 1988; p 334. (c) Rasing, T.; Berkovic, G.; Shen, Y. R.; Grubb, S. G.; Kim, M. W. *Chem. Phys. Lett.* **1986**, *130*, 1. (d) Heinz, T. F.; Tom, H. W. K.; Shen, Y. R. *Phys. Rev. A* **1983**, *28*, 1883.

(11) Zyss, J.; Chemla, D. S. In *Nonlinear Optical Properties of Organic Molecules and Crystals*; Chemla, D. S., Zyss, J., Eds.; Academic Press: New York, 1987; Vol. 1, p 23.

(12) Ye, P.; Shen, Y. R. *Phys. Rev. B* **1983**, *28*, 4288.

(13) (a) Hurst, M.; Munn, R. W. *J. Mol. Electron.* **1986**, *2*, 35, 43. (b) Munn, R. W. *J. Mol. Electron.* **1988**, *4*, 31.

(14) (a) Hurst, M.; Munn, R. W. In *Molecular Electronics-Science and Technology*; Aviram, A., Ed.; United Engineering Trustees: New York, 1990; p 267. (b) Hurst, M.; Munn, R. W. In *Organic Materials for Nonlinear Optics*; Hann, R. A., Bloor, D., Eds.; Royal Society of Chemistry: London, 1988; p 3. (c) Hurst, M.; Munn, R. W. *J. Mol. Electron.* **1987**, *3*, 75. (d) Hurst, M.; Munn, R. W. *J. Mol. Electron.* **1986**, *2*, 139.

(15) (a) Zyss, J.; Berthier, G. *J. Chem. Phys.* **1982**, *77*, 3635 (INDO and ab initio calculations of α, β, and γ for urea crystals). (b) Augspurger, J. D.; Dykstra, C. E. *Int. J. Quantum Chem.*, in press (ab initio and model calculations of α and γ for acetylene clusters). (c) Reference 6c (PPP level modelling of intermolecular β interactions for urea and prolinol-based chromophore crystals).

(16) (a) Zyss, J.; Chemla, D. S. *J. Chem. Phys.* **1981**, *74*, 4800. (b) Sigelle, M.; Hierle, R. *J. Appl. Phys.* **1981**, *52*, 4199.

(17) (a) Anderson, W. P.; Edwards, W. D.; Zerner, M. C. *Inorg. Chem.* **1986**, *25*, 2728. (b) Bacon, A. D.; Zerner, M. C. *Theor. Chim. Acta (Berlin)* **1979**, *53*, 21. (c) Ridley, J.; Zerner, M. C. *Theor. Chim. Acta (Berlin)* **1973**, *32*, 111.

(18) (a) Thompson, M. A.; Zerner, M. C. *J. Am. Chem. Soc.* **1991**, *113*, 8210–8215. (b) Thompson, M. A.; Zerner, M. C.; Fajer, J. *J. Phys. Chem.* **1991**, *95*, 5693–5700. (c) Canuto, S.; Zerner, M. C. *J. Am. Chem. Soc.* **1990**, *112*, 2114–2120.

(19) Ward, J. F. *Rev. Mod. Phys.* **1965**, *37*, 1.

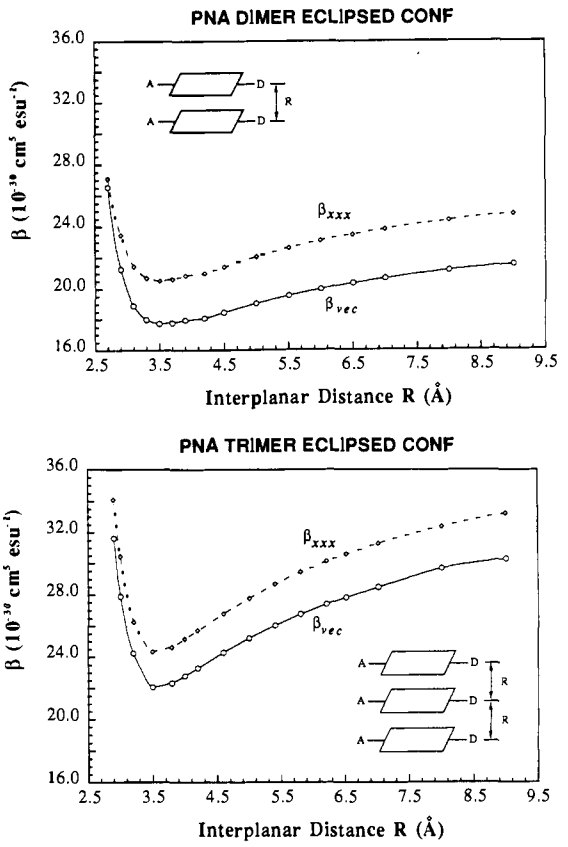

Figure 2. Variation of calculated hyperpolarizability components β_{vec} and β_{xxx} ($\hbar\omega$ = 0.65 eV) with interplanar distance (R) in a cofacial eclipsed PNA dimer (A) and trimer (B).

the 130 lowest energy transitions between SCF and MECI electronic configurations were chosen to undergo CI mixing and were included in the SOS. This SOS truncation was found to be sufficient for a complete convergence of the second-order response in all cases considered. Nevertheless, for a quantitative comparison of β_{ijk} values on passing from the monomer to the dimer and trimer in the eclipsed conformation, 160 states were included. For POM monomer, dimers and trimers, 180 and 270 states, respectively, were found to be sufficient for effective convergence of the SOS procedure.

Molecular Geometries

Geometrical parameters for calculations on monomeric PNA and POM molecules were taken from published crystallographic data,[20,21] assuming C_{2v} and C_s molecular symmetries, respectively. In all dimeric structures studied, the molecular geometries were constructed assuming each monomer to be planar, and systematically positioning them in various relative orientations. In the case of the PNA dimer, four different geometrical arrangements were considered (Figure 1). In the first, the dimer is in a cofacial eclipsed conformation (A). Starting from this conformation and holding the interplanar distance (R) at 3.5 Å, three additional molecular arrangements were considered. Staggered conformations (B) were generated by mutual rotation (α) of each molecular subunit; slipped conformations (C) were generated by parallel translations (R') along the x axis (C_x), and along the y axis (C_y), from the superimposed eclipsed structure; tilted conformations (D) were generated by increasing the dihedral angle α in the xy plane (D_x), alternatively keeping the donor–donor (R in D_{xD}) or the acceptor–acceptor (R in D_{xA}) distance constant, and along the y axis (D_y), keeping the C–C′ (R in D_y) distance between the two molecular subunits constant. The coordinate system was always chosen so that the resulting dimer molecular dipole moment was parallel to the x axis. For the POM dimer, only the eclipsed conformation (A) was considered. Finally, a model trimer in the eclipsed conformation (A) was also examined for both the PNA and POM molecules.

Table I. ZINDO-Derived Linear Optical Spectroscopic and Molecular Hyperpolarizability $\beta(-2\omega;\omega,\omega)$ Data (10^{-30} cm^5 esu^{-1}; $\hbar\omega$ = 0.65 eV) for the PNA Dimer in the Eclipsed Conformation at Various Interplanar Separations[a]

interplanar separation (Å)	$\hbar\omega_{ge}$[b] (eV)	f	$\Delta\mu$	$\beta_{t,xxx}$[c]	β_{xxx}
2.7	3.06	0.34	10.20	23.72	27.09
2.9	3.46	0.43	11.06	21.15	23.49
3.1	3.76	0.52	11.42	20.07	21.44
3.3	3.96	0.63	11.67	20.82	20.72
3.5	4.08	0.74	11.83	22.56	20.54
3.7	4.13	0.82	11.93	24.23	20.64
3.9	4.15	0.87	11.98	25.39	20.85
4.2	4.14	0.91	11.93	26.53	21.00
4.5	4.13	0.92	11.94	27.25	21.42
5.0	4.10	0.93	11.95	28.20	22.06
5.5	4.08	0.94	11.96	29.00	22.61
6.0	4.06	0.95	11.97	29.68	23.09
7.0	4.03	0.96	11.98	30.74	23.84
8.0	4.01	0.96	11.99	31.50	24.39
9.0	3.99	0.97	12.00	32.06	24.79
PNA[d]	3.90	0.48	11.78	16.04	12.29

[a] For definition of parameters, see text. [b] Lowest energy charge-transfer transition. [c] Calculated using the two-level model of eq 1. [d] Calculated for the PNA monomer. As a comparison, β_{vec}(calcd) = 10.6 × 10^{-30} cm^5 esu^{-1} versus β_{vec}(exper) = 9.2 × 10^{-30} cm^5 esu^{-1} ($\hbar\omega$ = 0.65 eV).[7b]

Results and Discussion

We first consider the simplest case represented by two monomeric units of PNA brought together in a cofacial eclipsed conformation (A) with dipolar axes aligned parallel to the x axis of the reference coordinate system. Figure 2A shows the dependence of β_{vec}[22] on the interplanar separation between the chromophore molecules. It reveals the importance of intermolecular π–π interactions in determining the nonlinear second-order optical response of such a system. At interplanar distances near 3.5 Å (corresponding to mean van der Waal's interactions in typical organic crystals), the curve reaches a flat minimum which increases asymptotically to a limiting value at larger distances (≥9.0 Å). This limiting value corresponds to approximately twice the calculated β value for the isolated chromophore (Table I). This result indicates, not surprisingly, that at large distances, the β response of individual molecules in such multimolecular systems becomes essentially independent of the surrounding molecules, and the second-order nonlinearity is an additive quantity. For distances smaller than 3.0 Å, the curve undergoes a sharp increase due predominantly to strong intermolecular dipole–dipole interactions. This result implies that hypothetical PNA dimers may exhibit large second-order NLO responses under extreme pressures. As expected, β_{xxx} is the largest component of the PNA dimer β_{ijk} tensor and exhibits the same trends with interplanar spacing as β_{vec} (Figure 2A); consequently, it dominates the nonlinear behavior, reflecting the pronounced one-dimensional character of the system. The other nonzero tensor components $\beta_{yyx} = \beta_{yxy}$ and β_{xyy} have smaller, negative values.

The above findings can be qualitatively rationalized in terms of the simple two-level model[23] for β (eq 1). Here β_t is a two-level

$$\beta_t(-2\omega;\omega,\omega) = \frac{3e^2}{2}\frac{\hbar\omega_{ge} f \Delta\mu_{ge}}{[(\hbar\omega_{ge})^2 - (\hbar\omega)^2][(\hbar\omega_{ge})^2 - (2\hbar\omega)^2]} \quad (1)$$

hyperpolarizability term, $\Delta\mu_{ge}$ is the difference between excited- and ground-state dipole moments, $\hbar\omega$ is the incident radiation frequency, $\hbar\omega_{ge}$ is the energy, and f is the oscillator strength of

(20) Trueblood, K. N.; Goldish, E.; Donohue, J. *Acta Cryst.* **1961**, *14*, 1009.
(21) Shiro, M.; Yamakawa, M.; Kubota, T. *Acta Cryst.* **1977**, *B37*, 1549.

(22) β_{vec} is given by

$$\beta_{vec}(-2\omega;\omega,\omega) = \sum^3_{i=1} \mu_i\beta_i/|\mu|$$

where $\beta_i = \beta_{iii} + {}^1/_3\sum_{j\neq i}(\beta_{ijj} + \beta_{jij} + \beta_{jji})$.
(23) (a) Oudar, J. L. *J. Chem. Phys.* **1977**, *67*, 446. (b) Oudar, J. L.; Chemla, D. S. *J. Chem. Phys.* **1977**, *66*, 2664.

Table II. ZINDO-Derived Molecular Hyperpolarizability β_{xxx} (10^{-30} cm^5 esu^{-1}; $\hbar\omega$ = 0.65 eV) Values for PNA and POM Monomers, and for PNA and POM Dimers and Trimers in the Eclipsed Conformation at an Interplanar Separation of 3.5 Å

	monomer	dimer[a]	trimer[a]
PNA	12.29	20.54 (24.58)	24.37 (36.87)
POM	−17.23	−31.77 (−34.46)	−43.75 (−51.69)

[a] Values in parentheses are calculated by the simple addition of monomer β_{xxx} values.

the optical transition ($\lambda_{max} = 2\pi c/\omega_{ge}$) involved in the two-level process. In the case where a charge-transfer transition has a major contribution along one molecular axis (e.g., the x axis), the β_t term should be largely proportional to the β_{xxx} tensor, so that $\beta_t(-2\omega;\omega,\omega) \cong \beta_{t,xxx}$. Table I compares, for selected interplanar distances, $\beta_{t,xxx}$ values calculated (input parameters are also compiled in Table I) via eq 1 with ZINDO-SOS β_{xxx} values. In each case, the estimated two-level $\beta_{t,xxx}$ terms approximate the SOS-derived β_{xxx} values reasonably well, so that the simplified analysis of variables influencing the geometry dependence of β_t is straightforward. For distances larger than 7.0 Å, the dimer molecular orbitals (MOs) are sums and differences of nearly unperturbed monomer molecular orbitals. This is reflected in both the calculated optical spectral features, which resemble those of the PNA monomer (Figure 3A,B), and in β_t values, which are about twice those of PNA (Table I).

On decreasing the interplanar distance, the relevant MOs are increasingly distorted, and orbital energies are shifted relative to monomer values. Consequently, the excited states cannot be expressed as a simple combination of monomer-like states, and the absorption spectrum is considerably modified (Figure 3C). In spite of this, the low energy, β-determining charge-transfer band remains unsplit and shifts to higher energies (Figure 3A–C) as is common for such cofacial interactions at these interplanar spacings[24] (qualitatively rationalizable in terms of through-space excitonic coupling model 3[24]), and the composition of the CI states

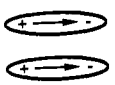

3

is again rather well described as a combination of the two highest occupied (HOMO) and the two lowest virtual (LUMO) MOs. This, accompanied by a gradual decrease in both $\Delta\mu$ and f values, leads to a decrease of β_t as the interplanar spacing is contracted. However, at distances less than 3.3 Å, the dipole–dipole interactions cause a strong energy splitting of each monomer-related MO with a resulting bathochromic shift of the calculated absorption spectra (Figure 3D).[25] This accounts well for the sharp increase of β_{xxx} (Figure 2, Table I). We also note that for larger interplanar distances, β_t values are overestimates of β_{xxx} because many monoexcited terms, other than β_t, also play an important role in the SOS perturbation.[7f] At such geometries, the two-level model is a relatively poor approximation.

The above trends in calculated β values are also observed in the analogous trimer of PNA having the same conformation and in the same range of interplanar distances (Figure 2B). A β minimum, somewhat more pronounced than found in the dimer, is observed at distances near 3.5 Å. This is another manifestation of how the intermolecular interactions, near equilibrium distances, become progressively stronger as the number of molecular subunits increases. In particular, on passing from the monomer, to the dimer and trimer, β_{xxx} values are 16% and 34% smaller than those estimated when considering the simple additivity of monomer β_{xxx}

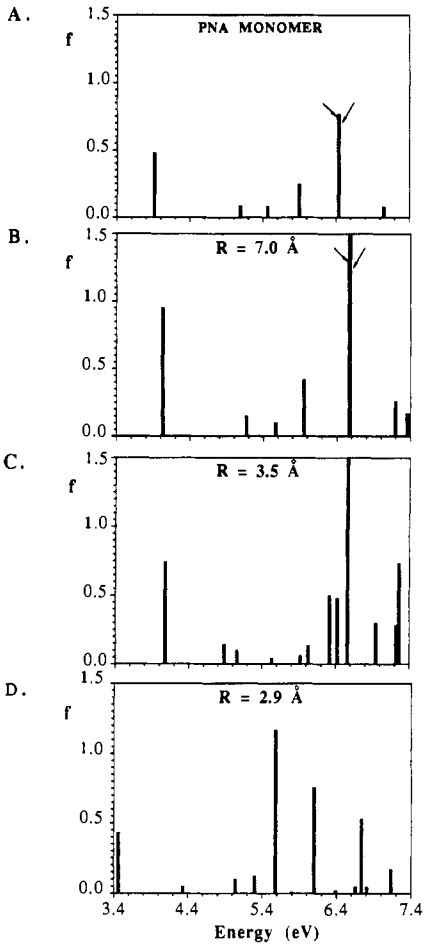

Figure 3. Calculated optical absorption spectra of the PNA dimer in the eclipsed conformation at various interplanar distances (R). The spectrum of the PNA monomer is also shown. The arrows indicate the superposition of two transitions.

values (Table II). Here the local field corrections (F) due to molecule–molecule interactions clearly begin to play a larger role in determining the macroscopic quadratic susceptibility, $\chi^{(2)}$.[11,13] In contrast, for larger interplanar distances (≥12.0 Å), the magnitude of β is again found to be an additive quantity. In this case, the local field correction is less important, as expected on simple electrostatic grounds.

The situation described above has been observed in chromophoric monolayers, where it has been found experimentally that for sufficiently small adsorbate molecular packing densities (N_s, in the range $1-3 \times 10^{14}$ molecules/cm^2), there is a linear relationship between the second-order optical susceptibility $\chi^{(2)}$ and N_s. In fact, assuming eq 2 for the $\chi^{(2)}$ tensor,[10] where $\langle T_{IJK}\rangle$ is

$$\chi^{(2)}_{IJK} = N_s F \langle T_{IJK}\rangle \beta_{xxx} \qquad (2)$$

a transformation matrix and β_{xxx} is the dominant component of the molecular hyperpolarizability, the observed linear dependence means that F is only weakly N_s-dependent, demonstrating that the local field corrections to molecule–molecule interactions are relatively unimportant in this regime.[10] Furthermore, by means of a classical point-dipole approximation, it has also been estimated that these local field effects should be negligible for distances between the adsorbate molecules larger than ~10 Å.[12] This agrees well with the present computational results.

The PNA dimer and trimer represent cases of a model built from strongly polar molecules, the dipole–dipole interactions of which strongly affect both the crystal structure and the NLO response.[26] It is now of interest to explore the opposite case of

(24) Ciliberto, E.; Doris, K. A.; Pietro, W. J.; Reisner, G. M.; Ellis, D. E.; Fragala', I.; Herbstein, F. H.; Ratner, M. A.; Marks, T. J. *J. Am. Chem. Soc.* **1984**, *106*, 7748, and references therein.

(25) In this case, similar to monomeric PNA, the composition of the CI state associated with the charge-transfer transition involves almost exclusively the HOMO and SLUMO MOs of the dimer.

(26) Nicoud, J. F.; Twieg, R. J. In *Nonlinear Optical Properties of Organic Molecules and Crystals*; Chemla, D. S., Zyss, J., Eds.; Academic Press: New York, 1987; Vol. 1, p 227.

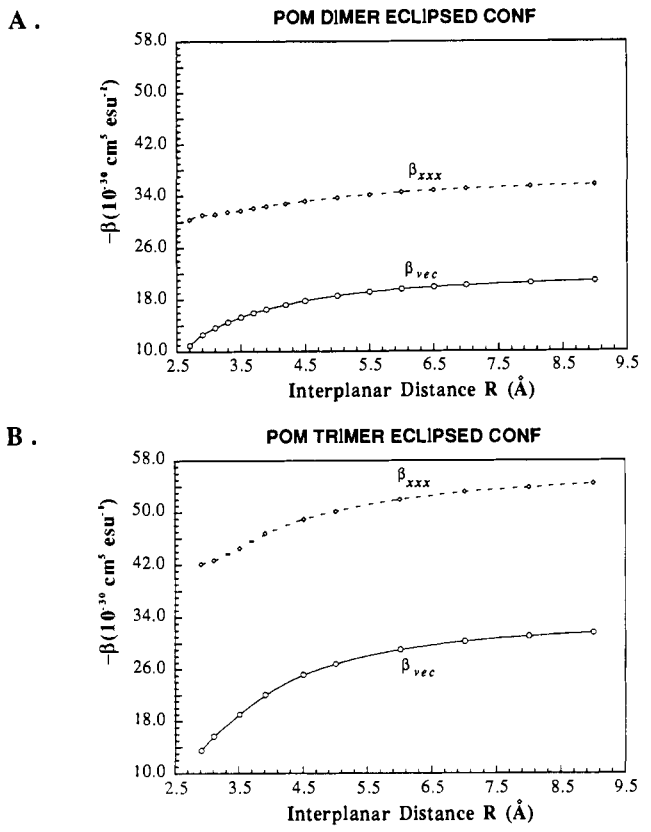

Figure 4. Variation of calculated hyperpolarizability β_{vec} and β_{xxx} components ($\hbar\omega$ = 0.65 eV) with interplanar distance (R) in a cofacial eclipsed POM dimer (A) and trimer (B).

a system constructed from molecular subunits with almost vanishing ground-state dipole moments such as POM (**2**).[27] The second-order NLO properties of this molecule are proposed to arise from a strong charge-transfer mechanism which leads to high negative $\Delta\mu$ and β values.[16a,28] The calculated β values for POM dimers in a cofacial eclipsed conformation are shown in Figure 4A. A significantly different, interplanar spacing-dependent trend in both β_{vec} and β_{xxx} values[29] is observed compared to the cofacial PNA dimer. In particular, the $\beta(R)$ curves lack a minimum and, on moving to larger distances, are slightly curved until ~6.0 Å, where they become nearly flat. Furthermore, β_{xxx} values at distances greater than 6.0 Å slightly but meaningfully exceed (in contrast to the PNA dimer) twice the calculated monomer β_{xxx} (Table III). This behavior may be again rationalized in terms of the previous two-level approach adopted for the PNA dimer. In particular, weak electrostatic molecule–molecule interactions (less than in PNA dimer) at relatively larger distances with consequent, nearly unperturbed ground and excited states, account well for the observed $\beta(R)$ trends. In fact, calculated spectral features for these distances are almost identical to those of the POM monomer (Table III, Figure 5A,B). At distances less than 3.7 Å, strong molecule–molecule interactions cause a complete modification of the calculated absorption spectra (Figure 5C,D). In these cases, the states are clearly dimeric, not merely excitonic

(27) (a) The reported experimental dipole moment of the parent 4-nitropyridine 1-oxide molecule is 0.69 D[27b] and compares well with the present calculated dipole moment (0.61 D). For the POM molecule, differing by a 3-methyl substituent, the calculated dipole moment is 1.16 D. (b) Katritzky, A. R.; Randall, E. W.; Sutton, L. E. *J. Chem. Soc.* **1957**, 1769.

(28) In the ground state, the *N*-oxide group behaves as an acceptor and the NO_2 as a donor; the resulting dipole moment is directed between the NO_2 and the CH_3 groups. In the excited states, there is an opposite situation: the *N*-oxide behaves as a donor and the NO_2 as an acceptor. Consequently, $\Delta\mu$ and in turn β are negative.

(29) In this case, since the total dipole moment and the molecular charge-transfer axis are not parallel (the charge transfer is directed along the D–A axis, while the resulting dipole moment is directed between the NO_2 and the CH_3 groups), β_{vec} values are consistently lower than β_{xxx}.

Table III. ZINDO-Derived Linear Optical Spectroscopic and Molecular Hyperpolarizability $\beta(-2\omega;\omega,\omega)$ Data (10^{-30} cm^5 esu^{-1}; $\hbar\omega$ = 0.65 eV) for the POM Dimer in the Eclipsed Conformation at Various Interplanar Separations[a]

interplanar separation (Å)	$\hbar\omega_{ge}$[b] (eV)	f	$\Delta\mu$	$\beta_{t,xxx}$[c]	β_{xxx}
2.7	3.26	0.25	−10.07	−13.78	−30.34
2.9	3.50	0.29	−10.62	−13.07	−31.09
3.1	3.68	0.33	−10.25	−12.19	−31.16
3.3	3.80	0.40	−9.11	−11.60	−31.42
3.5	3.80	0.54	−7.72	−13.22	−31.77
3.7	3.82	0.79	−9.22	−22.93	−32.09
3.9	3.82	0.92	−10.04	−29.17	−32.40
4.2	3.81	1.00	−10.56	−33.68	−32.80
4.5	3.80	1.04	−10.79	−35.97	−33.19
5.0	3.78	1.07	−10.96	−38.18	−33.74
5.5	3.77	1.09	−11.07	−39.72	−34.19
6.0	3.76	1.10	−11.11	−40.62	−34.55
7.0	3.75	1.11	−11.16	−41.96	−35.08
8.0	3.74	1.12	−11.19	−42.92	−35.48
9.0	3.73	1.13	−11.18	−43.30	−35.72
POM[d]	3.67	0.56	−10.91	−21.59	−17.23

[a] For definition of parameters, see text. [b] Lowest energy charge-transfer transition except for interplanar separations of 2.7–3.3 Å. In these cases, the second lowest (most intense) charge-transfer transition is given. [c] Calculated using the two-level model of eq 1. [d] Calculated data for the POM monomer.

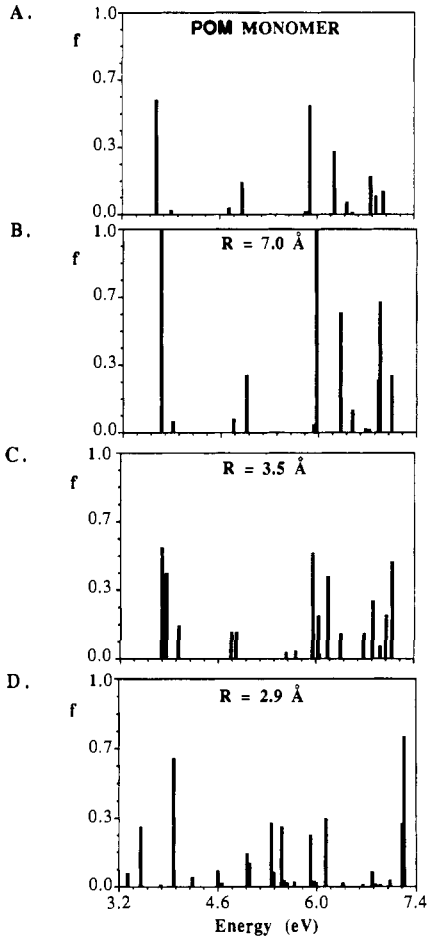

Figure 5. Calculated optical absorption spectra of the POM dimer in the eclipsed conformation at various interplanar distances (R). The spectrum of the POM monomer is also shown.

in character, and new charge-transfer bands appear at lower energies. In particular, the lower-energy charge-transfer transition is now split in two components, and the composition of the CI states cannot be simply described as a combination of two HOMOs and LUMOs. In addition, some transitions exhibit cross excitations. As a consequence, for smaller interplanar distances, the

simple two-level model accounts only qualitatively for $\beta(R)$ trends (Table III), since many low-energy excited states substantially contribute to the SOS-derived β_{xxx} values.

The above findings are fully confirmed in analyzing a model POM trimer in the same eclipsed conformation (Figure 4B). That is, for distances greater than 6.0 Å, the $\beta(R)$ curves are almost flat, and β_{xxx} values are approximately three times the POM monomer value. Furthermore, on passing from the monomer to the dimer and trimer (R = 3.5 Å), β_{xxx} values are 8% and 15% smaller, respectively, than those estimated from the additivity of the monomer β_{xxx} values (Table II). Therefore, the deviation from the simpler molecular β additivity model in determining the hyperpolarizability in POM clusters is smaller than in the PNA analogues. This implies that for assembled systems of POM chromophores, the local field corrections, except at very small distances, are almost negligible.

The observed differences in NLO response of the PNA and POM chromophore clusters is straightforward and may be explained in terms of differing intermolecular interactions.[30] In the PNA clusters, the intermolecular interactions are essentially electrostatic (dipole–dipole) in nature; at both large and small interplanar separations these dominate the other contributing interactions.[30b] The resulting excited states are hardly mixed (vide supra) although their energies are shifted by the relative amount of electrostatic interaction. Thus, the β response at various interplanar distances is largely determined (in a two-level picture) by the position of the lowest energy charge-transfer transition. In contrast, in the POM clusters, delocalization (or intermolecular charge-transfer) interactions[30b] operating only at short distances dominate the intermolecular interactions. Thus, while at short distances the relevant POM excited states are strongly mixed, leading to the anticipated breakdown of the two-level model, at relatively large distances, each molecule may be considered to be independent of the surrounding ones, giving an additive contribution to the hyperpolarizability.

The above analysis conveys interesting consequence for the molecular engineering of high-efficiency SHG thin-film materials. Using POM-like molecular precursors having small dipole moments, it should in principle be possible to assemble chromophoric layers cofacially having very high packing densities without appreciable reduction in molecular susceptibility. In fact, assuming eq 2 for the SHG $\chi^{(2)}$ response, $\chi^{(2)}$ becomes proportional to N_s. So increasing N_s affords a commensurately higher second-order NLO response. These results suggest that this analysis may be conveniently extended to other promising molecular systems in order to understand multimolecular NLO response in a macroscopic framework. Self-assembled[31] or adsorbed layer thin films,[32] for instance, seem the most suitable for this purpose. On the other hand, any geometrical distortion of the building blocks in an idealized molecular array is expected to play a role in modifying the macroscopic nonlinear response. However, if the type of distortion can be estimated, it can be readily taken into account in the calculations.

Let us now consider intermolecular intradimer tilt and the twist distortions which may be encountered in self-assembled multilayer films or in bulk crystals. Figure 6 shows the variation of β_{vec} values with mutual tilting of two initially cofacial PNA molecules. As expected, the D_y tilt leads to only small variations in β_{vec} (Figure 6A). In particular, larger tilt angles result in a small increase in β_{vec}. The maximum is found for α = 180°. This corresponds to a "fully coplanar" structure where both molecules are located in the xz plane. β_{xxx} is the largest component of the β_{ijk} tensor and parallels the $\beta_{vec}(R)$ curve. In contrast, $D_{xD,A}$ tilting, after a slight initial increase in β_{vec} for smaller angles, leads to a substantial falloff of β_{vec} for larger angles, finally reaching β_{vec} = 0 in the centrosymmetric "fully coplanar" (α = 180°) structures (Figure 6B). Futhermore, for larger tilt angles, the $\beta_{zzx} = \beta_{zxz}$ and β_{xzz} tensors, which are zero components for α = 0, dominate the nonlinear behavior.

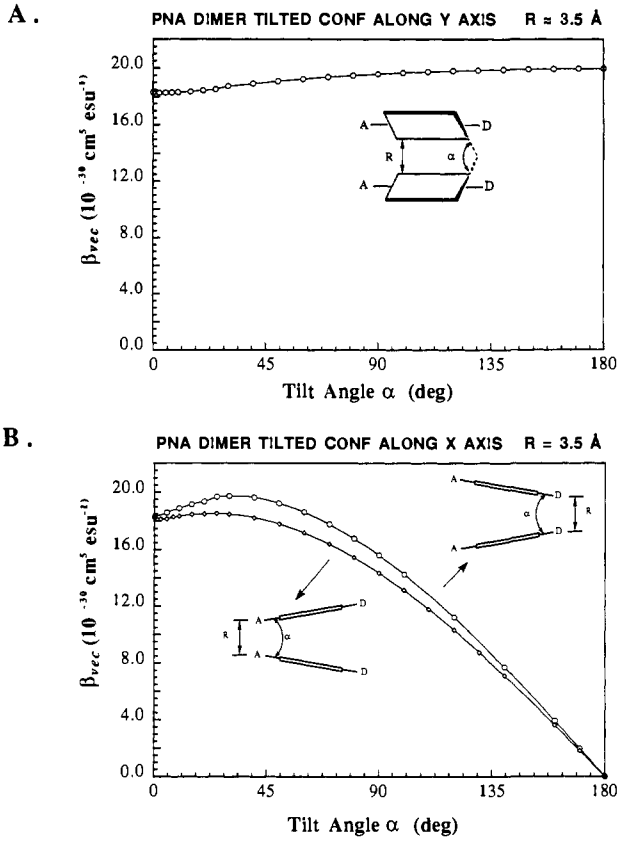

Figure 6. Variation of calculated hyperpolarizability β_{vec} component ($\hbar\omega$ = 0.65 eV) with tilt angle (α) along the y axis (A) and along the x axis (B) in PNA dimer (R = 3.5 Å).

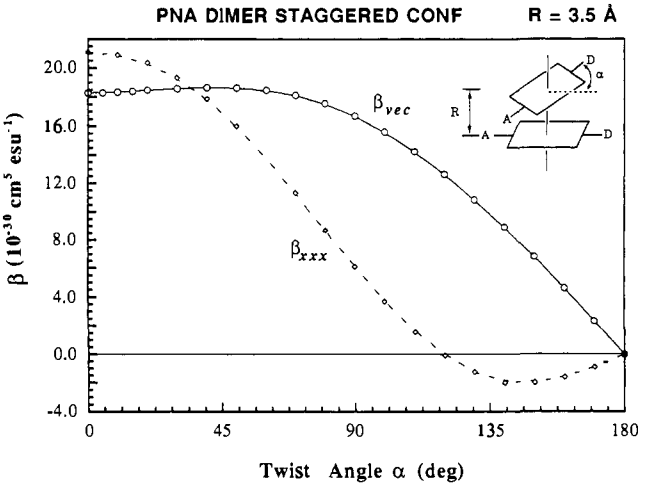

Figure 7. Variation of calculated hyperpolarizability β_{vec} and β_{xxx} components ($\hbar\omega$ = 0.65 eV) with twist angle (α) in the PNA dimer (interplanar distance R = 3.5 Å).

Turning to PNA dimers in various staggered conformations (structure B), it can be seen (Figure 7) that the β_{vec} curve is surprisingly flat for small to rather substantial staggering angles (<90°). For larger angles, β tends toward vanishing values as

(30) (a) Rigby, M.; Smith, E. B.; Wakeham, W. A.; Maitland, G. C. *The Forces Between Molecules*; Clarendon Press: Oxford, 1986; p 1. (b) Morokuma, K.; Kitaura, K. In *Molecular Interactions*; Ratajczak, H., Orville-Thomas, W. J., Redshaw, M., Eds.; Wiley: New York, 1980; Vol. 1, p 21.

(31) (a) Li, D.; Ratner, M. A.; Marks, T. J.; Zhang, C.; Yang, J.; Wong, G. K. *J. Am. Chem. Soc.* **1990**, *112*, 7389. (b) Ulman, A. *Adv. Mater.* **1990**, *2*, 573. (c) Allan, D. S.; Kubota, F.; Marks, T. J.; Zhang, T. J.; Lin, W. P.; Wong, G. K. *SPIE* **1991**, *1560*, 362. (d) Allan, D. S.; Kubota, F.; Orihashi, Y.; Li, D.; Marks, T. J.; Zhang, T. J.; Lin, W. P.; Wong, G. K. *Polym. Prepr.* **1991**, *32*, 86. (e) Allan, D. S.; Kubota, F.; Kakkar, A.; Marks, T. J.; Zhang, T. J.; Lin, W. P.; Shih, M.; Wong, G. K.; Dutta, P. *Mat. Res. Soc. Sympos. Proc.*, in press.

(32) (a) Tieke, B. *Adv. Mater.* **1990**, *2*, 222. (b) Barraud, A.; Vandevyver, M. In *Nonlinear Optical Properties of Organic Molecules and Crystals*; Chemla, D. S., Zyss, J., Eds.; Academic Press: New York, 1987; Vol. 1, p 357.

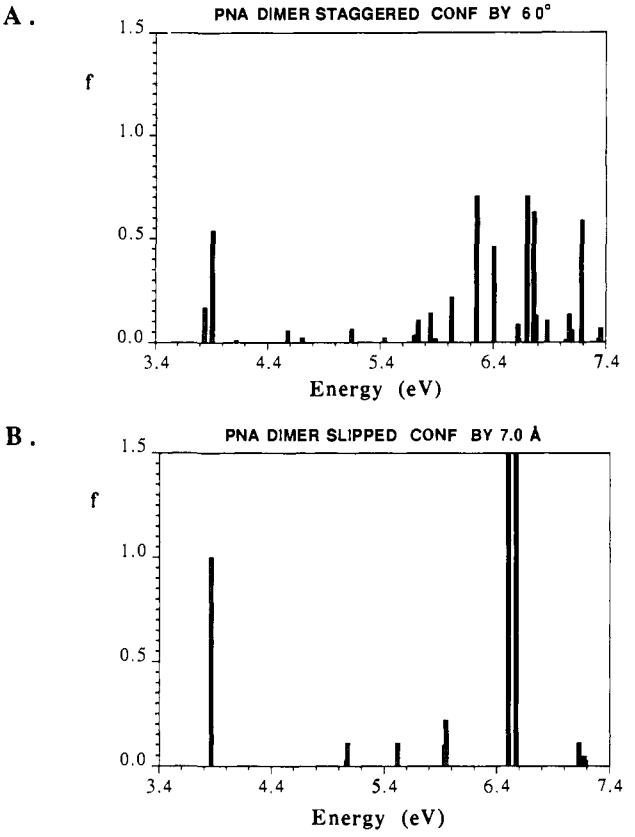

Figure 8. Calculated absorption spectrum of the PNA dimer in the staggered (α = 60°) (A), and in the slipped C_x (R' = 7.0 Å) (B) conformations (interplanar distance R = 3.5 Å). For a quantitative comparison with Figure 3, 160 states are considered.

the centrosymmetric (180°) conformation is approached. Thus, the β_{xxx} tensor, the principal hyperpolarizability component for smaller staggering angles, decreases precipitously with respect to the β_{vec} curve, so that for larger staggering angles, the other nonzero tensor components $\beta_{yyx} = \beta_{yxy}$ and β_{xyy} largely determine the nonlinear response. Due to symmetry lowering, the calculated absorption spectra of the twisted cofacial dimers are richer (compared to the analogous eclipsed dimer) as far as the number of transitions is concerned, and an additional transition appears at low energy (Figure 8A). Consequently, in this case, the simple two-level result is expected to be meaningfully in error, because several excited states contribute to the SOS β values.

The most dramatic cases of clustering-induced β enhancement occur in slipped cofacial conformations (C_x) where increasing slip distances are correlated with enhanced β values (Figure 9). A $\beta(R')$ maximum is found when the donor of a PNA unit lies approximately above the acceptor of the other molecule with 21% enhancement of calculated β_{xxx} values (β_{xxx} = 29.69, R' = 7 Å) with respect to those estimated from the simple monomer β additivity. In this arrangement, all the parameters which give rise to large β_t values (decreased ω_{ge}; increased f, $\Delta\mu$) are optimized (compared to the eclipsed conformation). The calculated absorption spectrum (Figure 8B) is similar to those of the PNA monomer and the PNA dimer in the eclipsed conformation at larger distances, as far as the number of transitions are concerned. However, the low-energy charge-transfer transition is red-shifted and the oscillator strength increased compared to those of the cofacial PNA dimers (Figures 8B, 3A–C). This indicates that small stabilizing dipole–dipole interactions (depicted in qualitative excitonic coupling terms as **4**) involving relevant MOs have only

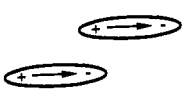

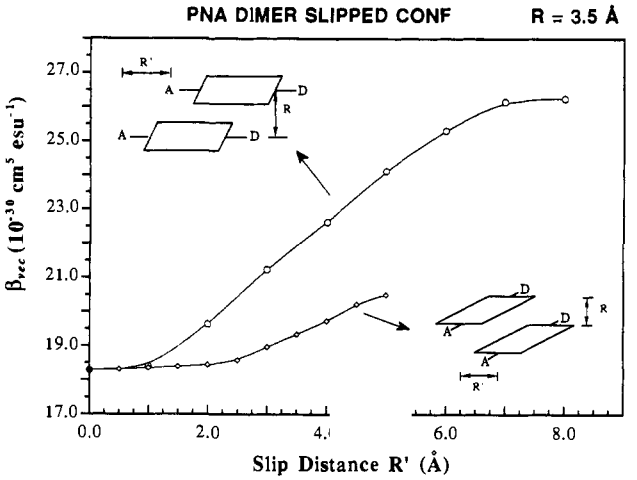

Figure 9. Variation of calculated hyperpolarizability β_{vec} component ($\hbar\omega$ = 0.65 eV) with slip distance (R') along the x and the y axes in the PNA dimer (interplanar distance R = 3.5 Å).

slightly distorted charge distributions and minimal contributions from the orbitals of the other subunit. The excited states may be characterized simply as linear combinations of monomer states. Consequently, the β response can be related to the additive contribution of each, nearly unperturbed molecular subunit further enhanced by the aforementioned red-shift of the low-energy charge-transfer transition (as easily deducible from eq 1). Qualitatively similar (but quantitatively diminished) behavior is also found in the case of C_y slip conformations where relatively larger β values are associated with increasing slip distances (Figure 9). In both cases, β_{xxx} is again the major component of the β_{ijk} tensor.

The interactions with the PNA dimer can, as already stated, be understood qualitatively in terms of a simple dipole–dipole interaction. For the interaction of two extended dipoles, as is appropriate for the PNA molecule, simple electrostatic arguments suggest that the interaction will decrease with the third power of the distance for initially superposed dipoles being separated along an axis perpendicular to the dipole moment. This is precisely what is observed in the lower line of Figure 9, where the curve begins to show some structure at R' = 3.5 Å, precisely where the change in the interaction should be manifested (for smaller distances, the R coordinate will dominate R' in the interdipole distance). For slippage of the dipoles along an axis parallel to the dipole moment, as occurs in the upper line of Figure 9, the description of the interactions is somewhat more complicated. Since these molecules are roughly 8 Å long, continuation of the upper curve in Figure 9 to even longer slip distances, R', would be expected to decrease the value of β_{vec}, until at a very, very large R', it approaches a value of roughly 21 × 10^{-30} cm^5 esu^{-1}, as suggested by Figure 2A. Calculations are underway to test the extent to which these simple dipole interaction models can be used, semiquantitatively, to understand the interactions in dimers of NLO chromophores.

Conclusions

The ZINDO model Hamiltonian is based on a minimum basis set of Slater orbitals, with many matrix elements defined semiempirically. Since it yields rather good agreement with experimental dipole moments, it should describe the electrostatic interactions in PNA dimers well, and since it is based on Slater orbitals, it seems appropriate for treatment of the long-range interactions needed to describe the POM dimers. While a number of important theoretical issues (neglect of multicenter exchange repulsion effects, possible role of basis set superposition error, adequacy of the semiempirical parameterization at long distances) must and will be addressed further in the context of comparison with careful, extensive ab initio studies, the results of the present study should still be of great value for understanding the effects of interchromophore interactions on β.[31] While dimer results (unlike those for monomers[7]) cannot be compared directly to

experiment, we anticipate that the qualitative pictures deduced from the present calculations will remain true in far more elaborate (and more computationally demanding) ab initio model Hamiltonians.

The present results show that intermolecular, chromophore–chromophore interactions can represent a major factor in determining the macroscopic second-order susceptibility of molecule-based NLO materials. The NLO response depends critically not only on the molecular packing geometries, but also significantly on the characteristics of the molecular constituents. At equilibrium chromophore–chromophore separations, the NLO response is a strong function of the relative molecular orientations. However, for relatively large intermolecular distances, particularly for component molecules having small ground-state dipole moments, each molecule may be considered to be independent of the surrounding ones, giving an additive contribution to the macroscopic susceptibility. Such effects find experimental counterparts in self-assembled or Langmuir–Blodgett thin films characterized by relatively low packing densities.[32,33] Thus, the optimization of packing density is clearly crucial for obtaining high-efficient SHG materials.

From the present results it can also be inferred that a bulk material having slipped (C_x) chromophore components would be expected to exhibit an optimum second-order nonlinearity. As a confirmatory example, 3-methyl-4-methoxy-4′-nitrostilbene (NMONS), the crystal structure of which consists of stacked π–π planar molecules in a slipped cofacial donor–acceptor (C_x-like) configuration (Figure 1), has one of the largest powder SHG efficiencies reported to date (1250 times more efficient than the urea).[34] High SHG signals are also observed from other substituted 4′-nitrostilbene derivatives which are stacked in a similar fashion,[35] and for the *N*-(4-nitrophenyl)-(L)-prolinol (NPP), the crystal structure of which consists of nearly planar molecules, in a C_x-like donor–acceptor configuration, connected by an infinite network of hydrogen-bonded chains.[36] In these cases, favorable angles between molecular charge-transfer axes (or favorable dipolar orientations within the unit cell)[8] also render these crystals well suited for efficient phase-matching.[35,36]

Finally, the two-level model, extensively used for the qualitative prediction of molecular hyperpolarizabilities, is not of general validity for calculations on chromophore clusters. In fact, for large chromophore–chromophore distances, it overestimates β. At normal chromophore–chromophore equilibrium distances, the two-level model is still valid; however, in the case of strongly delocalized intermolecular interactions, it also fails to reliably predict the hyperpolarizability.

Acknowledgments. This research was supported by the NSF-MRL program through the Material Research Center of Northwestern University (Grant DMR8821571) and by the Air Force Office of Scientific Research (Contract 90-0071). S.D.B. thanks the Italian Consiglio Nazionale delle Ricerche (CNR, Rome) for a postdoctoral fellowship. We thank Professor M. C. Zerner for providing us with the ZINDO code and Dr. D. R. Kanis for numerous helpful discussions.

Registry No. 1, 100-01-6; **2**, 1074-98-2.

(33) A recent study (Itoh, Y.; Hamada, T.; Kakta, A.; Muko, A. *SPIE Proc.* **1990**, *1337*, 293) presents some important but preliminary β results for 4-nitro-3-methylaniline in an ab initio calculation. Their results are in good qualitative agreement with ours.

(34) (a) Tam, W.; Guerin, B.; Calabrese, J. C.; Stevenson, S. H. *Chem. Phys. Lett.* **1989**, *154*, 93. (b) Bierlein, J. D.; Cheng, L. K.; Wang, Y.; Tam, W. *Appl. Phys. Lett.* **1990**, *56*, 423.

(35) Grubbs, B. R.; Marder, S. R.; Perry, J. W. *Chem. Mat.* **1991**, *3*, 3.

(36) Zyss, J.; Nicould, J. F.; Coquillay, M. *J. Chem. Phys.* **1984**, *81*, 4160.

Energetics, Proton Transfer Rates, and Kinetic Isotope Effects in Bent Hydrogen Bonds

Xiaofeng Duan and Steve Scheiner*

Contribution from the Department of Chemistry and Biochemistry, Southern Illinois University, Carbondale, Illinois 62901. *Received January 6, 1992*

Abstract: N—H···N H-bonds which occur in intermolecular contacts and in intramolecular situations where the bond is bent are investigated by ab initio methods. Distortion of the θ(N—H···N) angle of up to 40° from linearity results in modest increases in the barrier to proton transfer while a much higher barrier occurs in $NH_2CH_2NH_3^+$ where this angular distortion is some 100°. The rate of transfer is orders of magnitude slower in the latter system. In contrast to earlier suppositions that systems containing nonlinear H-bonds are subject to smaller kinetic isotope effects, k_H/k_D for the most highly strained system is larger than in the other complexes. This distinction is attributed in part to the difference in zero-point vibrational energies but primarily to the contribution of tunneling. Not only the value of k_H/k_D but also the temperature sensitivity of this parameter is enhanced by nonlinearity of the H-bond.

Introduction

Decades of experimental study of the proton transfer reaction in solution have yielded a rich harvest of information concerning mechanisms, reaction rates, and sensitivity of pK to solvent type.[1,2] More recent developments in techniques have permitted the reaction to be studied in the gas phase, free of the many complicating effects of a bulk-phase solvated environment.[3-7] It is also possible in this manner to separate the energetic and entropic factors involved in the reaction of each pair of molecules. Details about the molecular geometry associated with proton transfer have been harder to come by. Microwave measurements in the gas phase

(1) Caldin, E. F.; Gold, V. *Proton Transfer Reactions*; Halsted: New York, 1975.

(2) Stewart, R. *The Proton: Applications to Organic Chemistry*; Academic: Orlando, 1985.

(3) Cheshnovsky, O.; Leutwyler, S. *J. Chem. Phys.* **1988**, *88*, 4127. Knochenmuss, R.; Cheshnovsky, O.; Leutwyler, S. *Chem. Phys.* **1988**, *144*, 317.

(4) Dodd, J. A.; Baer, S.; Moylan, C. R.; Brauman, J. I. *J. Am. Chem. Soc.* **1991**, *113*, 5942.

(5) Meot-Ner, M.; Smith, S. C. *J. Am. Chem. Soc.* **1991**, *113*, 862.

(6) Meot-Ner, M. *J. Am. Chem. Soc.* **1989**, *111*, 2830-2834.

(7) Hierl, P. M.; Ahrens, A. F.; Henchman, M.; Viggiano, A. A.; Paulson, J. F.; Clary, D. C. *J. Am. Chem. Soc.* **1986**, *108*, 3140.

0002-7863/92/1514-5849$03.00/0